

SCIENTIFIC REPORTS



OPEN

Predicting Growth and Carcass Traits in Swine Using Microbiome Data and Machine Learning Algorithms

Christian Maltecca¹, Duc Lu¹, Constantino Schillebeeckx², Nathan P. McNulty¹ ², Clint Schwab³, Caleb Shull³ & Francesco Tiezzi¹

In this paper, we evaluated the power of microbiome measures taken at three time points over the growth test period (weaning, 15 and 22 weeks) to foretell growth and carcass traits in 1039 individuals of a line of crossbred pigs. We measured prediction accuracy as the correlation between actual and predicted phenotypes in a five-fold cross-validation setting. Phenotypic traits measured included live weight measures and carcass composition obtained during the trial as well as at slaughter. We employed a null model excluding microbiome information as a baseline to assess the increase in prediction accuracy stemming from the inclusion of operational taxonomic units (OTU) as predictors. We further contrasted performance of models from the Bayesian alphabet (Bayesian Lasso) as well machine learning approaches (Random Forest and Gradient Boosting) and semi-parametric kernel models (Reproducing Kernel Hilbert space). In most cases, prediction accuracy increased significantly with the inclusion of microbiome data. Accuracy was more substantial with the inclusion of microbiome information taken at weeks 15 and 22, with values ranging from approximately 0.30 for loin traits to more than 0.50 for back fat. Conversely, microbiome composition at weaning resulted in most cases in marginal gains of prediction accuracy, suggesting that later measures might be more useful to include in predictive models. Model choice affected predictions marginally with no clear winner for any model/trait/time point. We, therefore, suggest average prediction across models as a robust strategy in fitting microbiome information. In conclusion, microbiome composition can effectively be used as a predictor of growth and composition traits, particularly for fatness traits. The inclusion of OTU predictors could potentially be used to promote fast growth of individuals while limiting fat accumulation. Early microbiome measures might not be good predictors of growth and OTU information might be best collected at later life stages. Future research should focus on the inclusion of both microbiome as well as host genome information in predictions, as well as the interaction between the two. Furthermore, the influence of the microbiome on feed efficiency as well as carcass and meat quality should be investigated.

The efficiency of producing saleable meat products is primarily determined by costs associated with feed and by the amount of and quality of lean meat produced^{1,2}. Utilizing feed resources more efficiently has become a definite challenge that faces the livestock industry. Recent efforts have been devoted to identifying and exploiting the genomic variability of individual pigs in increasing feed efficiency³⁻⁵. Despite its success, this approach presents logistical as well as technical limitations related to obtaining accurate individual feed intake records⁶ as well as defining and using different feed efficiency measures⁷. Perhaps most importantly, a continued effort concentrating only on the pig variability for efficiency would inevitably lead to diminished marginal gains, incurring in concomitant losses of overall fitness and genetic diversity over time^{8,9}. The amount and type of bacteria present in the gut of individuals represent a key part of all mammalian organisms¹⁰. The makeup of the microbiome

¹North Carolina State University, Animal Science Department, Raleigh, 27695, USA. ²Matatu Inc., Saint Louis, 63108, USA. ³The Maschhoffs LLC, Carlyle, 62231, USA. Christian Maltecca, Duc Lu and Francesco Tiezzi contributed equally. Correspondence and requests for materials should be addressed to C.M. (email: cmaltec@ncsu.edu) or F.T. (email: f_tiezzi@ncsu.edu)

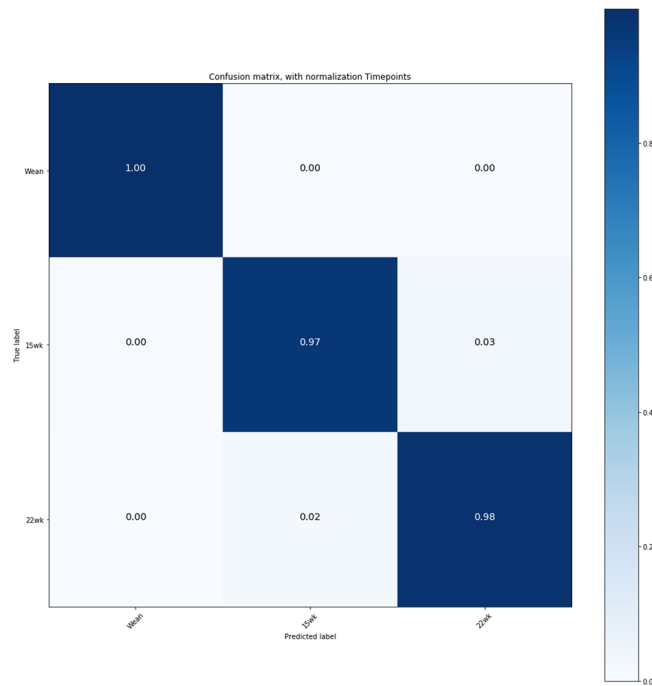


Figure 1. Normalized classification confusion matrix of microbiome composition at three time points. *Wean* = Weaning, *15wk* = 15 weeks, *22wk* = 22 weeks. Confusion matrix obtained with an RF model from a five-fold cross-validation.

represents a vast pool of genomic diversity that contributes to physiology and health¹¹. Particularly, the intestinal microbiome directly affects the degradation of carbohydrates, provides short-chain fatty acids, mitigates and alter the effect of potentially toxic compounds and produces essential vitamins¹². The impact of environmental factors, such as nutrition^{13,14} stressors, and challenges associated with weaning^{15,16} and management^{17,18} have been characterized in pigs. Nonetheless, the composition and function of a healthy microbial ecosystem have not been qualitatively and quantitatively defined and used as a tool to maximize animal health and performance¹⁹. Particularly, microbiome composition has yet to be studied at large scales, including large sampling conducted through several stages of production²⁰. Within this paper, we assessed the power of microbiome predictions based on fecal samples, to foresee growth and carcass composition in a population of healthy crossbred pigs. In doing so, we employed machinery typical of host genomic predictions, including models of the Bayesian alphabet as well as semi-parametric and machine learning algorithms.

Results

Within this work we evaluated the effectiveness of longitudinal microbiome data to inform prediction of growth and carcass composition in swine. For this purpose, we employed and contrasted models that have been proven successful in the genomic selection arena in order to provide the blueprint for the future routine inclusion of microbiome information in selection programs. We evaluated the performance of the proposed models in a cross-validation setting. We further tested the overall experimental design with a mixed model based post-analysis.

Microbiome composition over time. The distribution of taxonomic abundances for the three time points measured (weaning, 15 weeks, and 22 weeks) in the current population has been described in detail recently by Lu and colleagues¹⁹. Since the objective of the current paper was not to provide the ecological landscape of the population measured, the reader is referred to that paper for more details. Briefly, at the three different stages of pig development, there were 14, 21, 29, 54, 106, and 202 identified phyla, classes, orders, families, genera, and species, respectively. For the three sampling points, 95.79–97.80% of the OTUs were classified into six phyla: Firmicutes, Bacteroidetes, Proteobacteria, Fusobacteria, Spirochaetes, and Actinobacteria. Bacteria that were in the phylum Firmicutes represented the majority of the total population followed by Bacteroidetes. To evaluate the ability of the microbiome to predict phenotypic measures, we conducted a preliminary analysis to investigate how different sampling times affected fecal microbiome composition. To do so, we fitted a random forest model similar to the one employed for growth and carcass traits (see Methods), with the only difference that in this case the model was used to classify each observation into one of the three sampling times. We report the results of the five-fold classification in Fig. 1, which depicts the normalized classification confusion matrix at weaning, 15 weeks and 22 weeks. Individual time measurements constituted three distinct microbial populations. The accuracy of classification was in all cases extremely high (>95%). The misclassification rate was marginally higher for 15 wk and 22 wk (~3%). This result is in line with a report by Lu and colleagues¹⁹ which identified two distinct microbial enterotypes at weaning but less distinct clustering at later time points. Additional information can be

found in supplemental material, where abundance over time (Supplementary Fig. 1), principal coordinate analysis (Supplementary Fig. 2) and significant log fold changes of families at different time points (Supplementary Fig. 3) are reported.

Cross-validation highlights a significant effect of microbiome for growth and carcass prediction.

We first evaluated the power of microbiome data in predicting several growth parameters in a healthy population of crossbred sires originating from the mating of 28 founding sires' families. For this purpose we considered: weights, back fat, loin area and depth traits measured at 14 and 22 weeks of a growth trial as well as daily gain measures for the same period. These were coupled with fecal microbiome information obtained for the same individuals at weaning as well as week 15 and 22 of the trial. Each trait was analyzed independently using a cross-validation scheme, in which some samples' phenotypes and OTUs were employed to train the statistical models, and the remainder were used to validate the predictions. We considered three classes of models in the analyses: one model from the Bayesian alphabet family, Bayesian Lasso (BL)²¹; two machine learning approaches, Random Forest (RF)²² and Gradient Boosting Machine (GBM)²³; and one semi-parametric method, Reproducing Kernel Hilbert Space (RKHS)²⁴. We chose these models as representative of the most widely used methods for genomic prediction in livestock and crops. We have done this to emphasize the similarity of the analyses proposed in the current work to genomic selection approaches, both in scope and methodology, as well as to provide a baseline to expand upon, with the inclusion of genomic information in future comparisons.

Figs 2, 3 and 4 report the accuracies of prediction for each trait, fecal microbiome time point, and method combination. Microbiome contribution to prediction was measured as deviation from a null model which included only the effects of sex, sire, weight at weaning, and replicate. It should be noted that the null model was fitted in all cases within each of the algorithms proposed. For ease of comparison, null models performance is represented as the average of null models across methods. Inclusion of OTU abundances in the prediction models increased accuracies in most instances with respect to the null model. Nonetheless, the amount varied according to the microbiome time point. In general, the inclusion of microbiome composition at weaning had low predictive power for daily gain traits as well as carcass measures obtained at week 15 and 22 (Fig. 2). For daily gain traits (panel A), the inclusion of microbiome information increased accuracies of prediction by ~3%, yet in all cases, 90% CI of the prediction (panel C) overlapped between the null and the biom models, for all algorithms employed. Daily gain in later stages of the trial was better predicted than early growth, regardless of the inclusion of microbiome information. Similar trends were observed for carcass traits measured at weeks 14 and 22, with predictions ranging from ~15% for loin depth (panels B, C), to ~40% for back fat, for both null and OTU models. Conversely, microbiome composition at week 15 substantially increased accuracy in the test sets (Fig. 3). The amount was dependent on the trait/time combination. In general, and as expected, microbiome composition increased prediction accuracies more for traits measured concomitantly with the microbiome sampling. For daily gain traits (panel A) the inclusion of microbiome information increased the accuracy of prediction of early growth from ~20% for the null model for daily gain from birth to week 14 and from weaning to week 14 to ~40 and 45% for the same two traits. Similarly, for all traits measured at week 14 (panel B), microbiome information boosted prediction accuracy significantly, with gains of ~0.20 for weight and back fat and ~0.05 and 0.10 for loin depth and area, respectively. Similar trends were seen for week 22 traits, albeit with smaller increases and with overlapping 90% CI (panel D) for several of the traits, with the exception of weight. Figure 4 depicts results of cross-validation predictions for microbiome measured at week 22. It should be noted that given the temporal succession of sampling, combinations of phenotypes measured at week 14 and microbiome at week 22 should be interpreted with caution due to the temporal succession of the measures. Again, for most traits microbiome information increased prediction accuracy. Yet, for most trait/model combinations the increase was not significant. Specifically, and focusing on week 22 traits, only weight and back fat benefited from including OTU with gains of ~0.08 for back fat and ~0.05 for weight. Interestingly, including OTU abundances did not increase accuracy of prediction for later daily gains traits (from week 14 to week 22 and from week 14 to market).

The results presented are in line with what has been observed in other studies. He and colleagues²⁵ found that swine gut microbiome had a moderate effect on fat with microbiome explaining from 1.5% to 2.73% phenotypic variance for average back fat and abdominal fat weight, respectively. Similarly, Fang and colleagues²⁶ found 119 OTUs associated with intramuscular fat in growing pigs. Furthermore, McCormack *et al.*²⁷ identified several gut microbes potentially associated with porcine feed efficiency and Yang and colleagues²⁸ identified two potential enterotypes in Duroc pigs associated with residual feed intake. Data on daily gain and weight is more sparse yet, for example, Ramayo *et al.*²⁹ identified clusters of piglets based on OTU abundance, significantly associated with body weight at 60 d and average daily gain. It is worth noting that in most cases these studies focused on either the identification of ecological populations of bacteria or the identification of specific OTUs associated with a particular phenotype. To the best of our knowledge, this is the first attempt to rigorously characterize the overall predictive ability of the microbiome for growth and carcass traits in swine, and livestock in general. In our analysis in most cases the inclusion of microbiome composition data boosted prediction accuracy beyond what expected by the identification of few important taxonomical units, not dissimilarly from what observed in genomic predictions in several livestock species³⁰, suggesting a more complex interconnection between different OTUs and microbiome compositions than highlighted in previous studies. Furthermore, a growing body of literature exists pointing to a rich interplay between the pig and its metagenome^{19,31}. This represents both a challenge and an opportunity to incorporate microbiome information in selection programs effectively. The microbiome could potentially be considered an entirely environmental source of variation but also one at least partially under the direct control of the host. The methods employed in the current analysis would prove extremely flexible in integrating the full spectrum of variability generated by the availability of microbiome and host genomic data. Some of these approaches could be applied directly following GxE examples in both plants and livestock^{32,33}.

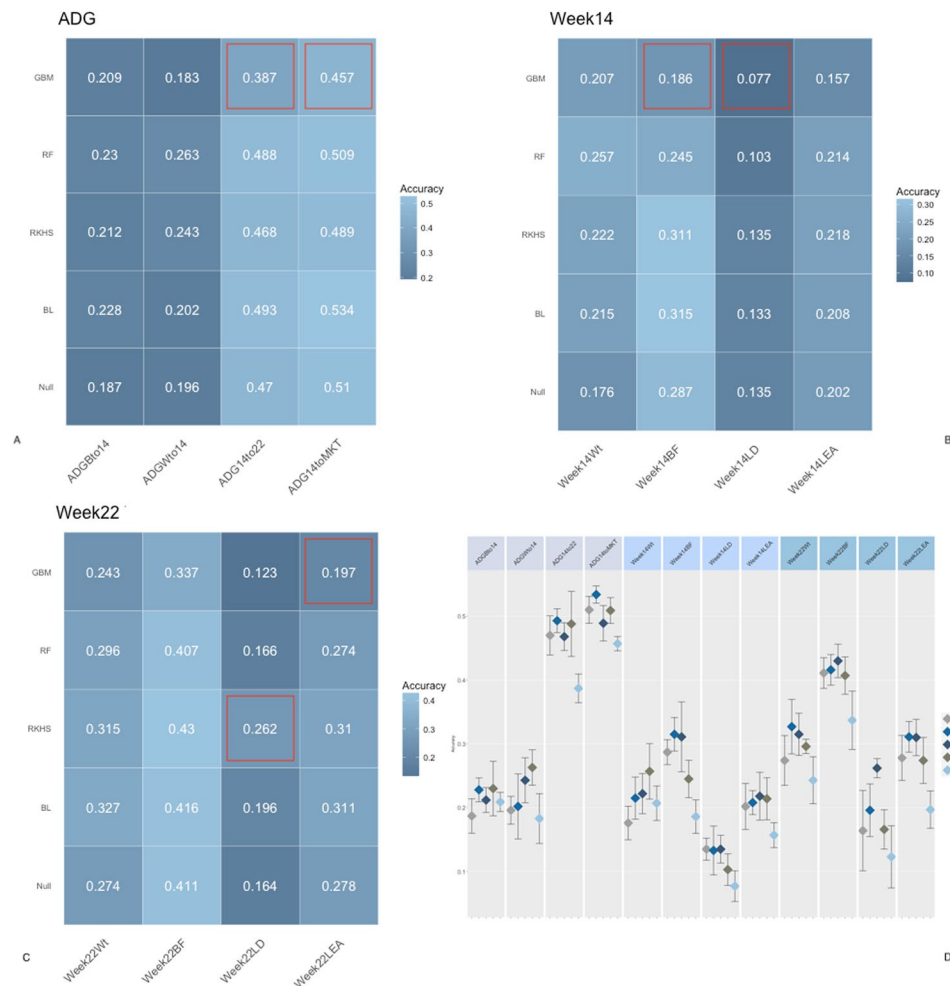


Figure 2. Accuracy of prediction for microbiome composition at Weaning. Panel (A) Accuracy for daily gain traits, Panel (B) Accuracy for Week 14 traits, Panel (C) Accuracy for Week 22 traits, Panel (D) 90% confidence interval for model/trait combinations. Confusion matrix obtained with a RF model from a five-fold cross-validation. *BL* = Bayesian Lasso, *RF* = Random Forest, *GBM* = Gradient Boosting Machine, *RKHS* = Reproducing Kernel Hilbert Space. *ADGBto14* = Average Daily Gain Birth to week14, *ADGWto14* = Average Daily Gain Weaning to week14, *ADG14to22* = Average Daily Gain week14 to week22, *ADG14toMKT* = Average Daily Gain week 14 to Market, *Week14Wt* = weight at week14, *Week14BF* = backfat at week14, *Week14LD* = loin depth at week14, *Week14LEA* = loin eye area at week14, *Week22Wt* = weight at week22, *Week22BF* = backfat at week22, *Week22LD* = loin depth at week22, *Week22LEA* = loin eye area at week22. Red outlines indicate prediction significantly different from null model.

Model choice partially influences prediction accuracy, with results depending on the time-trait combination.

We investigated the effectiveness of different model classes to incorporate microbiome information for the prediction of growth and carcass phenotypes in pigs. We chose models ranging from completely, to semi, to non-parametric to recognize and possibly capture the complex interdependent structure of OTUs compositions. The models were tested independently for each trait time point combination. We evaluated the performance by comparing models including microbiome composition to a baseline model including only general design factors (see Methods). Bayesian Lasso is one model of the “Bayesian Alphabet”³⁴ family, that has gained popularity in genomic selection due to its ability to effectively handle large p small n problems in genomic prediction as well as providing a framework for feature selection. BL was proposed by Xu *et al.*²¹ and de los Campos *et al.*²¹. We chose it as one of the most robust and popular choices in the parametric class of models. Reproducing Kernel Hilbert Space is a particularly flexible class of semi-parametric models that have been proposed to fit complex multidimensional data. They have recently gained popularity in livestock and crop breeding thanks to the work of Gianola and colleagues³⁵ and of de los Campos *et al.*³⁶. Models of this class rely on the choice of an appropriate kernel that is then employed in models of form not dissimilar from the mixed models commonly employed in breeding settings. Random Forest is an ensemble method fitting decision trees on various sub-samples of the dataset³⁷. Random forest models are generally robust to over-fitting and can capture complex interaction structures in the data³⁸. Gradient Boosting is an alternative ensemble method²³ aimed at combining predictors, in this case in a sequential manner, by forming committees of predictors with higher predictive ability than single ones.

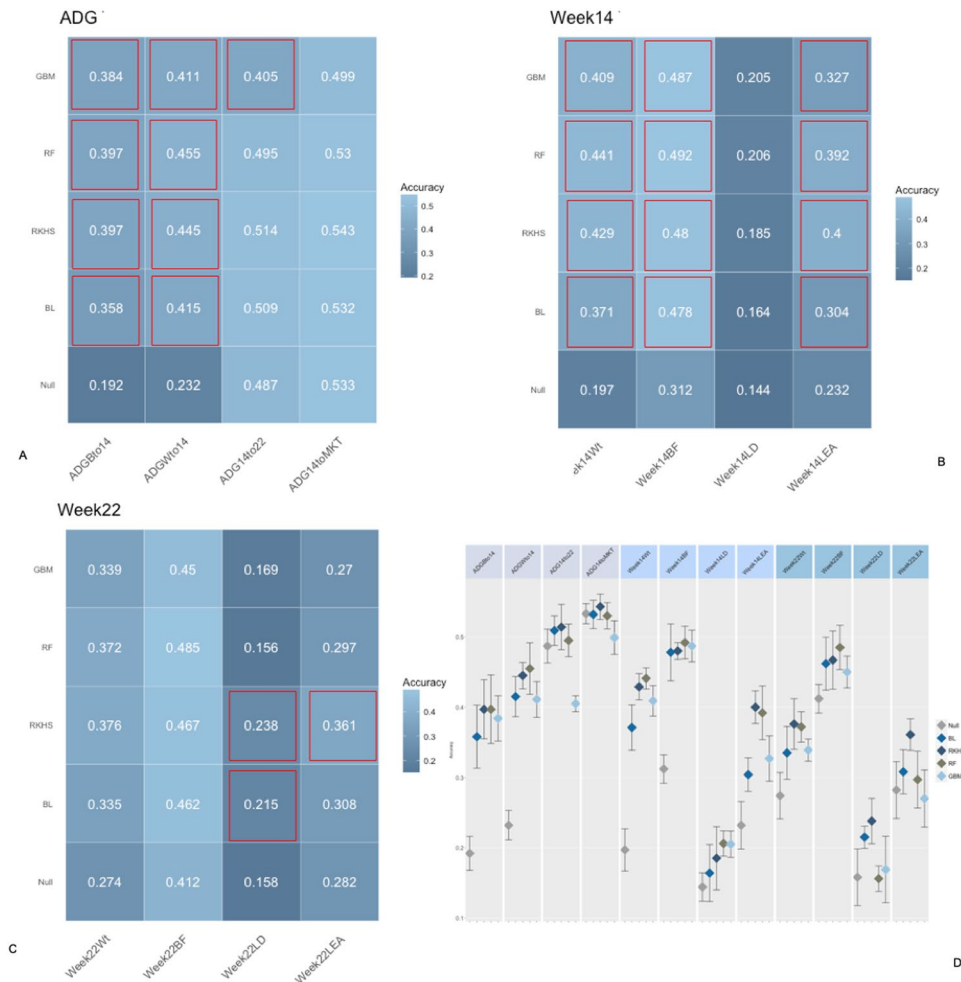


Figure 3. Accuracy of prediction for microbiome composition at Week 15. Panel (A) Accuracy for daily gain traits, Panel (B) Accuracy for Week 14 traits, Panel (C) Accuracy for Week 22 traits, Panel (D) 90% confidence interval for model/trait combinations. Confusion matrix obtained with a RF model from a five-fold cross-validation. *BL* = Bayesian Lasso, *RF* = Random Forest, *GBM* = Gradient Boosting Machine, *RKHS* = Reproducing Kernel Hilbert Space. *ADGBto14* = Average Daily Gain Birth to week14, *ADGWto14* = Average Daily Gain Weaning to week14, *ADG14to22* = Average Daily Gain week14 to week22, *ADG14toMKT* = Average Daily Gain week14 to Market, *Week14Wt* = weight at week14, *Week14BF* = backfat at week14, *Week14LD* = loin depth at week14, *Week14LEA* = loin eye area at week14, *Week22Wt* = weight at week22, *Week22BF* = backfat at week22, *Week22LD* = loin depth at week22, *Week22LEA* = loin eye area at week22. Red outlines indicate prediction significantly different from null model.

Panel D of Figs 3, 4 and 5 portrays point estimates and 90% CI for each model-trait combination. In the vast majority of cases, the choice of model was a wash. In our analysis we weren't able to identify a clear winner, and for the most part models' CIs largely overlapped. Reproducing Kernel Hilbert Space models emerged as the most stable approach across scenarios in terms of ranking and magnitude of the CI, followed by Bayesian Lasso and Random Forest, while Gradient Boosting showed the largest variation in performance across trait times. At weaning gradient boosting models in some cases performed worse than the null model. This is unsurprising though, as in most cases microbiome data at weaning contributed little to the learning of the models. Our results are similar to what has been observed for the prediction of complex traits with genomic information in both plants³⁹ and in livestock^{40,41}, where different classes of models performed similarly over a wide variety of conditions so that in most cases the choice of model is somewhat more dependent on population and data structure than that the underlying biological signal. It is important to note that while for DNA polymorphism-informed predictions marker information is somewhat, (loosely speaking) a fixed parameter, OTU composition can be much more variable across both individuals and experimental settings, due to variability in sampling procedures, environmental conditions, as well as the bioinformatic machinery employed in obtaining taxonomical units. While we do recognize that some of this variability cannot be effectively managed through statistical modeling, we also believe that some of these models might be more flexible in handling such sources of variation. This should be the subject of further investigation, and it is beyond the scope of the current paper. Within this work and in recognition of this complexity, we attempted to overcome some of these limitations by obtaining prediction accuracies

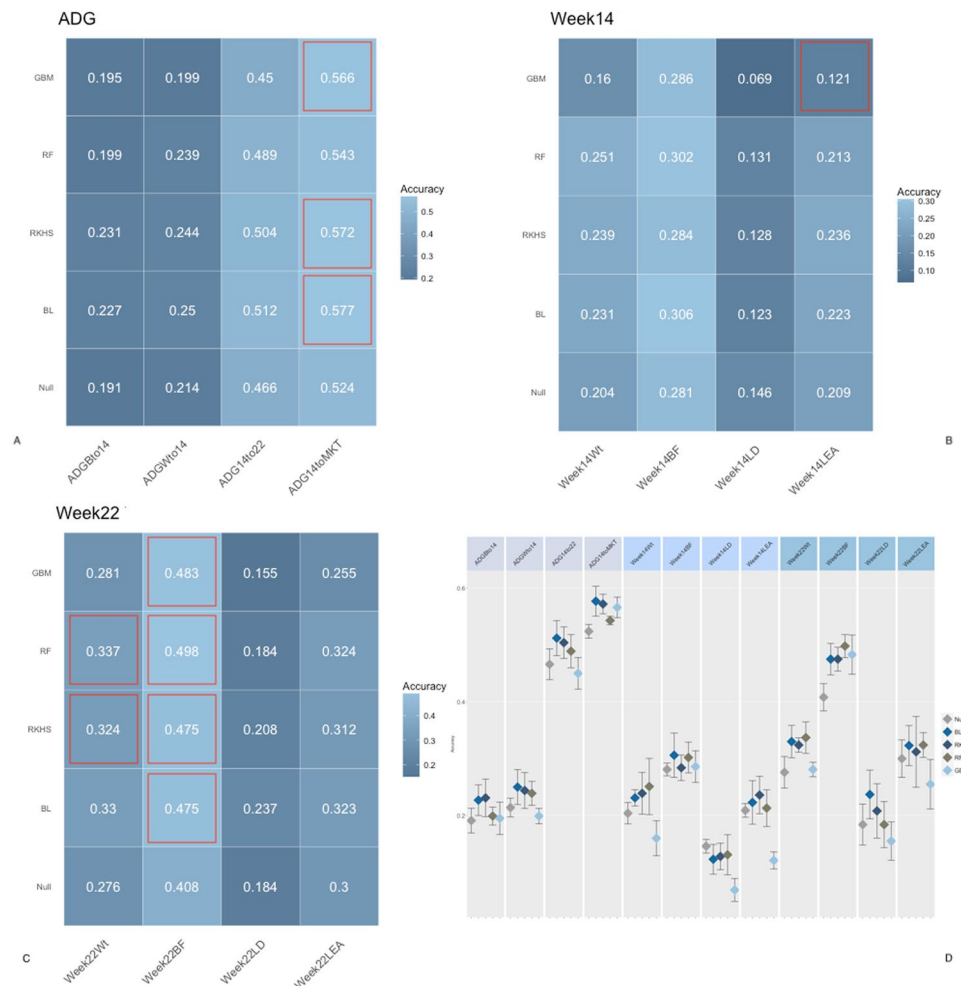


Figure 4. Accuracy of prediction for microbiome composition at Week 22. Panel (A) Accuracy for daily gain traits, Panel (B) Accuracy for Week 14 traits, Panel (C) Accuracy for Week 22 traits, Panel (D) 90% confidence interval for model/trait combinations. Confusion matrix obtained with a RF model from a five-fold cross-validation. *BL* = Bayesian Lasso, *RF* = Random Forest, *GBM* = Gradient Boosting Machine, *RKHS* = Reproducing Kernel Hilbert Space. *ADGBto14* = Average Daily Gain Birth to week14, *ADGWto14* = Average Daily Gain Weaning to week14, *ADG14to22* = Average Daily Gain week14 to week22, *ADG14toMKT* = Average Daily Gain week14 to Market, *Week14Wt* = weight at week14, *Week14BF* = backfat at week14, *Week14LD* = loin depth at week14, *Week14LEA* = loin eye area at week14, *Week22Wt* = weight at week22, *Week22BF* = backfat at week22, *Week22LD* = loin depth at week22, *Week22LEA* = loin eye area at week22. Red outlines indicate prediction significantly different from null model.

averaged across models. Results from this analysis were obtained by pooling information across replicate and methods and are presented in Fig. 6. Results in this case are presented with two competing models, a null model (obtained again pooling null fit across methods) and a microbiome model (biom) obtained by averaging the performance of each trait/method combination. Results for the most part recapitulate what is presented in the previous section. In some cases, differences between null and microbiome model have shrunk (e.g. for week 22 back fat). Mean Squared Errors (MSE) for the competing trait/model combinations are reported in Table 1. Results recapitulate for the most part the ones for accuracy with MSE generally lower for the models including microbiome information, particularly for wk15 and wk22 and models performance that varied with trait/time-point. Differences in most cases, though, were more nuanced compared to the null model and in some cases (e.g. Week14Wt and Week22Wt), microbiome models did not perform significantly better in terms of MSE compared to the null models. Thus, results for some comparisons should be interpreted with caution, and further studies with a larger sample size should be performed.

Post-analysis of the results. We attempted to evaluate the overall influence of all factors in the design on predictive performance with a post-analysis of the cross-validation study. To do so we employed a standard LMM approach (see Methods) and obtained least square mean estimates and contrasts for all variables in the analysis. Namely we fitted the effect of the inclusion of microbiome information, the algorithm used for the analysis, the time point at which the fecal microbiome was sampled, the trait analyzed and all the pairwise interactions. The

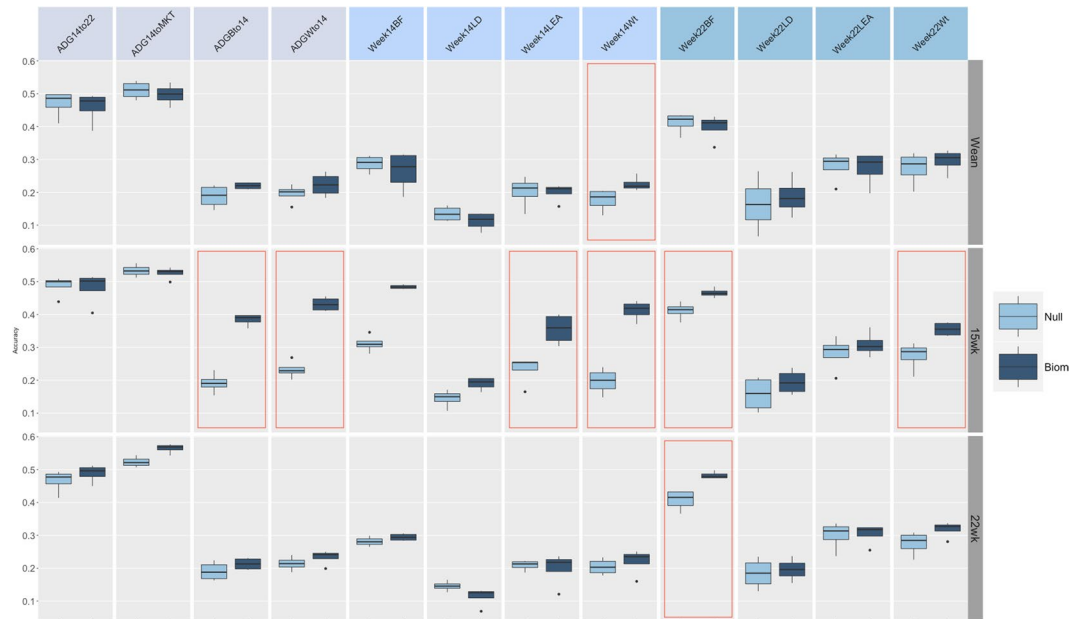


Figure 5. Model Average accuracy of prediction for microbiome composition at Weaning week 14 and week 22. *Null* = Average of null models. *Biom* = Average of Microbiome models. *ADGBto14* = Average Daily Gain Birth to week14, *ADGWto14* = Average Daily Gain Weaning to week14, *ADG14to22* = Average Daily Gain week14 to week22, *ADG14toMKT* = Average Daily Gain week14 to Market, *Week14Wt* = weight at week14, *Week14BF* = backfat at week14, *Week14LD* = loin depth at week14, *Week14LEA* = loin eye area at week14, *Week22Wt* = weight at week22, *Week22BF* = backfat at week22, *Week22LD* = loin depth at week22, *Week22LEA* = loin eye area at week22. Red outlines indicate prediction significantly different from null model.

response variable was in this case the accuracy of prediction in the cross-validation experiment. Results of this investigation are reported in Table 2 and Fig. 7. Table 2 reports the Type III ANOVA of the overall experimental design. All factors and their interactions were highly significant with the exception of the interaction between Algorithm and Trait. The interaction between algorithm and time point was also just below the $P < 0.05$ significance threshold. Figure 7 depicts the least square means of the significant main effects and their interactions. The inclusion of microbiome data (averaged over all other factors) increased the prediction ability of models by approximately 4% over the null model (0.321 vs. 0.281). Of the models considered, and as seen in the previous sections, GBM was the one with the lowest predictive ability (0.26) while RKHS was the one with the highest predictive power (0.32), although nearly identical to Bayesian Lasso and Random Forest algorithms. Microbiome information collected at week 15 had the highest predictive power (0.335) compared to weaning which had the lowest. Differences between the first and the two latter were ~5% and ~4%, respectively. Daily gain traits and back fat traits were the best predicted, while loin traits, both area and depth, had the lowest accuracies. The Interaction between different models and the inclusion of microbiome data shows once again that RKHS models performed best regardless of the presence of microbiome data. Interestingly both Random Forest and Gradient Boosting were the algorithms that gained the most from the inclusion of OTU information, with improvements versus the null model of ~5% in both cases. Similar trends were observed for the time point-algorithm interaction. Finally, the interaction of microbiome information with time points highlight how, in our data, microbiome information collected at week 15 largely outperforms (~10%) all other time point (as well as null models). To the best of our knowledge, this is the first attempt to formally assess microbiome predictions in livestock. Comparable models have been used with human microbiome data to predict disease⁴², and with soil microbiome data to predict crop yield⁴³. In both cases, the use of microbiome data improved predictive power, but given the vast diversity of both scope and measures, it is difficult to draw a direct comparison.

Discussion

In general, our cross-validation highlighted good predictive power, however results varied considerably depending on the time points and traits considered. From our study it appears that sampling time might be a crucial factor in integrating microbiome information in predictive models for growth. Our data suggest that samples measured in the middle of the growth trial would provide the highest amount of information. Conversely early measures of microbiome composition might not be as informative. This is somewhat in contrast with recent studies^{28,29} that have found different enterotypes related to growth traits at earlier stages. In our experience, and as highlighted by Lu *et al.*¹⁹, clustering of individuals at early time points could be the results of piglet adjusting more or less rapidly to the change in diet that normally happens at weaning. We believe this should be investigated further. Within this paper we considered the study of each time point as separate and independent. This is a simplification that us allowed to build an easy cross-validation experiment to test different variables. Nonetheless, the use of longitudinal models in the future would provide a much more powerful way to investigate the importance

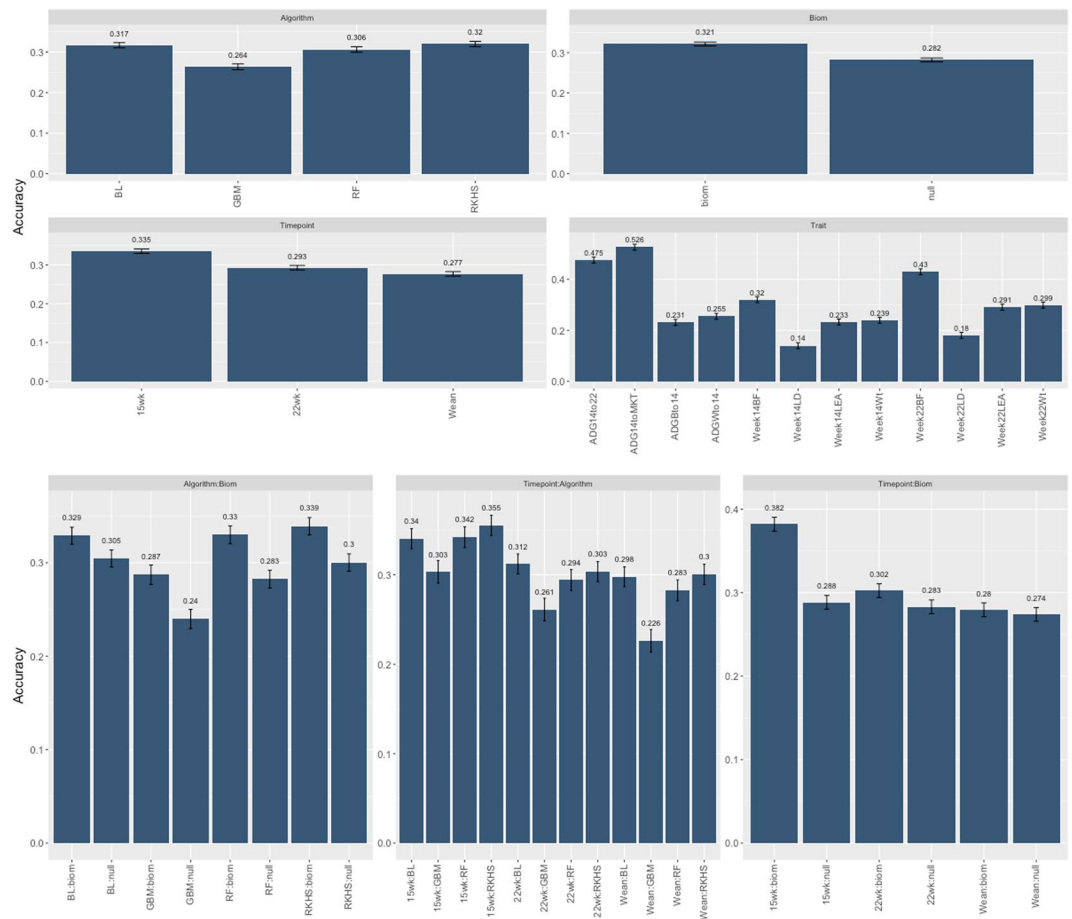


Figure 6. Least Square Means and SE for main effects and interactions for the post-analysis of the experimental design. *Timepoint* = 3 levels (Weaning, 15 weeks, 22 weeks), *Algorithm* = 4 levels (Bayesian Lasso, Reproducing Kernel Hilbert Space, Random Forest, Gradient Boosting Machine) *Trait* = 12 levels (“ADGBto14”, “ADGWto14”, “ADG14to22”, “ADG14toMKT”, “Week14Wt”, “Week14BF”, “Week14LD”, “Week14LEA”, “Week22Wt”, “Week22BF”, “Week22LD”, “Week22LEA”), *Biom* = 2 levels (null, microbiome). All elements with (:) represent pairwise interactions.

of changes in microbiome composition, and how these changes impact growth efficiency in livestock. To this point, some of the deep learning models developed in the context of prediction of longitudinal data⁴⁴ should allow for a much better understanding of the complex interplay between changes in microbiome composition and phenotype outcome. Nonetheless, a much larger number of individuals as well as deeper sampling would be needed to reach the necessary data granularity to make these approaches appealing. In our studies both growth traits and fatness traits achieved good predictive power. Furthermore, the current study was conducted within a single crossbred population. For the effective exploitation of microbiome variability in pigs a larger number of populations/breeds should be investigated, given the large variability in OTU composition in swine⁴⁵. Within this work we have established a framework that could later be expanded to include not only microbiome information but also host genomic data⁴⁶, to better characterize and possibly manage the environment as well as to account for the complex relationships between host and guest variability. Microbiome composition can be effectively used as a predictor of growth and composition traits, particularly for fatness traits. Inclusion of OTU predictors could potentially be used to promote fast growth of individuals while limiting fat accumulation. Early microbiome measures might not be good predictors of growth and OTU information might be best collected at later life stages. It should be noted that within the current paper we have included microbial composition as a whole predictor, and we did not attempt to identify a significant OTU subset to reduce the space of the predictors. We believe that this approach would result in more robust and portable results especially for selection purposes. Nonetheless more information on individual OTUs significantly associated with each combination of time/trait is reported in supplemental material (Supplementary Table 1)

Methods

Animals. The pigs used in this study were grown in a commercial setting operated by The Maschhoffs LLC (Carlyle, IL, USA). Animal use approval was therefore not needed for the data collection. Offspring for the current study originated from twenty-eight purebred Duroc sires, from a Duroc population under selection for lean growth, mated to Large White × Landrace or Landrace × Large White sows. The resulting offspring were weaned

Method	Trait	MSE (Wean)	SD (Wean)	MSE (14 wk)	SD (15 wk)	MSE (22 wk)	SD (22 wk)
Null	ADGBto14	0.032	0.002	0.032	0.002	0.032	0.002
BL		0.032	0.002	0.028	0.002	0.031	0.002
RKHS		0.031	0.003	0.027	0.001	0.031	0.002
RF		0.031	0.002	0.029	0.003	0.032	0.001
GBM		0.034	0.001	0.029	0.002	0.035	0.003
Null	ADGWto14	0.044	0.003	0.044	0.002	0.044	0.002
BL		0.044	0.004	0.041	0.005	0.043	0.005
RKHS		0.042	0.003	0.035	0.003	0.042	0.002
RF		0.040	0.003	0.038	0.004	0.042	0.003
GBM		0.048	0.004	0.037	0.001	0.047	0.001
Null	ADG14to22	0.096	0.006	0.096	0.006	0.097	0.005
BL		0.091	0.008	0.097	0.008	0.092	0.007
RKHS		0.096	0.007	0.091	0.008	0.090	0.009
RF		0.096	0.004	0.091	0.005	0.095	0.007
GBM		0.108	0.007	0.107	0.008	0.097	0.007
Null	ADG14toMKT	0.068	0.006	0.068	0.001	0.066	0.002
BL		0.066	0.008	0.067	0.001	0.060	0.002
RKHS		0.068	0.005	0.068	0.002	0.061	0.002
RF		0.064	0.006	0.067	0.002	0.066	0.005
GBM		0.079	0.007	0.071	0.006	0.061	0.003
Null	Week14Wt	492.4	29.12	492.3	48.37	493.7	36.75
BL		490.3	38.01	402.9	22.97	461.2	37.40
RKHS		471.1	19.83	381.6	32.58	467.3	38.03
RF		458.7	43.82	417.2	40.81	471.6	19.54
GBM		509.6	15.21	426.6	34.53	522.6	33.57
Null	Week14BF	0.011	0.000	0.012	0.000	0.012	0.001
BL		0.011	0.001	0.011	0.001	0.012	0.001
RKHS		0.011	0.001	0.010	0.001	0.011	0.001
RF		0.011	0.001	0.010	0.001	0.011	0.001
GBM		0.013	0.001	0.010	0.001	0.012	0.001
Null	Week14LD	0.037	0.002	0.036	0.003	0.035	0.001
BL		0.038	0.004	0.037	0.002	0.034	0.002
RKHS		0.036	0.001	0.034	0.001	0.035	0.002
RF		0.035	0.003	0.034	0.001	0.034	0.002
GBM		0.041	0.002	0.037	0.002	0.039	0.002
Null	Week14LEA	0.501	0.047	0.495	0.013	0.489	0.037
BL		0.475	0.017	0.482	0.035	0.446	0.023
RKHS		0.48	0.025	0.429	0.018	0.479	0.024
RF		0.484	0.035	0.467	0.043	0.461	0.022
GBM		0.573	0.014	0.459	0.037	0.585	0.028
Null	Week22Wt	840.59	72.62	841.57	76.63	849.17	42.45
BL		794.52	67.09	771.92	18.20	770.12	43.67
RKHS		806.89	29.13	789.51	60.79	789.23	33.99
RF		789.13	33.59	773.37	49.07	792.02	37.89
GBM		928.37	55.37	855.15	33.41	847.26	49.75
Null	Week22BF	0.037	0.003	0.038	0.001	0.038	0.002
BL		0.036	0.004	0.037	0.002	0.036	0.004
RKHS		0.036	0.002	0.035	0.003	0.036	0.002
RF		0.035	0.002	0.036	0.002	0.035	0.003
GBM		0.043	0.003	0.036	0.002	0.036	0.004
Null	Week22LD	0.043	0.005	0.042	0.002	0.042	0.002
BL		0.041	0.004	0.042	0.004	0.039	0.003
RKHS		0.040	0.005	0.038	0.004	0.041	0.005
RF		0.041	0.001	0.04	0.002	0.042	0.003
GBM		0.049	0.004	0.044	0.004	0.044	0.004
Continued							

Method	Trait	MSE (Wean)	SD (Wean)	MSE (14 wk)	SD (15 wk)	MSE (22 wk)	SD (22 wk)
Null	Week22LEA	0.734	0.055	0.742	0.056	0.718	0.049
BL		0.711	0.026	0.735	0.035	0.668	0.033
RKHS		0.693	0.021	0.685	0.070	0.698	0.078
RF		0.717	0.031	0.706	0.062	0.719	0.041
GBM		0.833	0.047	0.781	0.078	0.785	0.069

Table 1. Mean squared error average and standard deviation for each combination of Trait/Model/ Age Category for a 5-fold cross validation. BL = Bayesian Lasso, RF = Random Forest, GBM = Gradient Boosting Machine, RKHS = Reproducing Kernel Hilbert Space. *ADGBto14* = Average Daily Gain Birth to week14, *ADGWto14* = Average Daily Gain Weaning to week14, *ADG14to22* = Average Daily Gain week14 to week22, *ADG14toMKT* = Average Daily Gain week14 to Market, *Week14Wt* = weight at week14, *Week14BF* = backfat at week14, *Week14LD* = loin depth at week14, *Week14LEA* = loin eye area at week14, *Week22Wt* = weight at week22, *Week22BF* = backfat at week22, *Week22LD* = loin depth at week22, *Week22LEA* = loin eye area at week22.

	Sum Sq	Mean Sq	F value	Pr (>F)
Timepoint	0.272	0.136	87.637	0.000***
Algorithm	0.270	0.090	57.937	0.000***
Trait	8.889	0.593	381.430	0.000***
Biom	0.281	0.281	180.905	0.000***
Timepoint:Algorithm	0.020	0.003	2.164	0.047*
Timepoint:Trait	0.258	0.009	5.543	0.000***
Timepoint:Biom	0.148	0.074	47.746	0.000***
Algorithm:Trait	0.083	0.002	1.186	0.208
Algorithm:Biom	0.027	0.009	5.900	0.001**
Trait:Biom	0.287	0.019	12.311	0.000***

Table 2. ANOVA table of the post-analysis of the experimental design. *Timepoint* = 3 levels (Weaning, 15 weeks, 22 weeks), *Algorithm* = 4 levels (Bayesian Lasso, Reproducing Kernel Hilbert Space, Random Forest, Gradient Boosting) *Trait* = 12 levels (“ADGBto14”, “ADGWto14”, “ADG14to22”, “ADG14toMKT”, “Week14Wt”, “Week14BF”, “Week14LD”, “Week14LEA”, “Week22Wt”, “Week22BF”, “Week22LD”, “Week22LEA”), *Biom* = 2 levels (null, microbiome). All rows with (:), represent pairwise interactions.

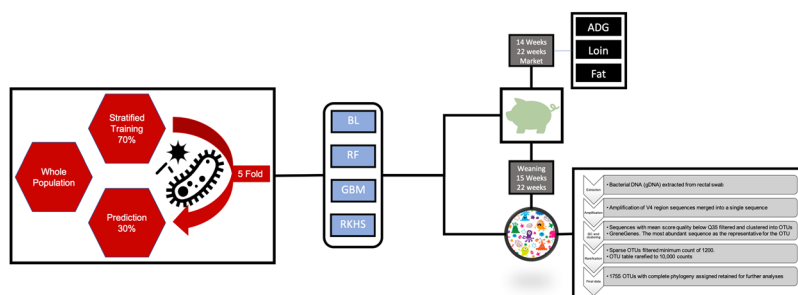


Figure 7. Overall Experimental design. BL = Bayesian Lasso, RF = Random Forest, GBM = Gradient Boosting, RKHS = Reproducing Kernel Hilbert Space. ADG = Average Daily Gain.

at 18.6 days (± 1.09) and subsequently moved to a nursery-finishing facility. Here individuals were grouped in batches of 20 pigs per pen. Pen mates were paternal half-siblings of the same gender and similar weaning weight. We performed six replicates of this basic experimental block, each composed of 2 pens (one pen of female and one pen of castrated male pigs) from each of the 28 sires. The test period began the day the pigs entered the nursery-finishing facility. Individuals were fed a standard pellet diet during nursery, growth, and finish periods. Diet formulations and their nutritional values are provided [see Additional file 1]. The pigs received a standard vaccination and medication routine [see Additional file 2]. End of test was reached on a pen-specific basis when all pigs in a pen achieved an average live weight of 136 kg. Their average age at harvest was 196.4 days (± 7.86). We collected rectal swabs from all pigs in a pen at three time points: weaning, 15 weeks post weaning (average 118.2 ± 1.18 days, hereafter “wk15”), and 22 weeks post weaning (average 196.4 days ± 7.86 days, hereafter “wk22”). Four pigs were chosen randomly per pen for lean carcass growth measurements, and their rectal swabs

	Min	Max	Mean	SD
ADGBto14 (kg/d)	0.26	0.81	0.57	0.08
ADGWto14 (kg/d)	0.26	0.93	0.64	0.10
ADG14to22 (kg/d)	0.20	1.40	0.86	0.16
ADG14toMKT (kg/d)	0.29	1.30	0.89	0.14
Week14Wt (kg)	31.71	98.30	68.78	9.88
Week14BF (cm)	0.58	2.29	1.25	0.28
Week14LD (cm)	2.52	5.64	4.24	0.48
Week14LEA (cm ²)	12.64	41.35	28.38	4.57
Week22Wt (kg)	81.99	154.47	117.26	13.37
Week22BF (cm)	0.84	4.24	2.00	0.53
Week22LD (cm)	4.01	7.29	5.59	0.52
Week22LEA (cm ²)	27.55	63.74	43.90	5.69

Table 3. Summary of phenotypes used in the study. *ADGBto14* = Average Daily Gain Weaning to week14, *ADGWto14* = Average Daily Gain Weaning to week14, *ADG14to22* = Average Daily Gain week14 week22, *ADG14toMKT* = Average Daily Gain week14 to Market, *Week14Wt* = weight at week14, *Week14BF* = backfat at week14, *Week14LD* = loin depth at week14, *Week14LEA* = loin area at week14, *Week22Wt* = weight at week22, *Week22BF* = backfat at week12, *Week22LD* = loin depth at week22, *Week22LEA* = loin area at week22.

were used for microbiome sequencing. In the end, the number of samples at weaning, week 15, and week 22 were 1205, 1295, and 1283, respectively. There were 1039 animals with samples collected at all 3 time points. More details on the distribution of samples across families, time points, and sex are provided [see Additional file 3]. Loin depth, loin area as well as back fat thickness and weights were recorded on live animals at weeks 14 and 22 post-weaning and at market weight. These measures will be hereafter referred to as Week14LEA, Week14LD, Week14BF, Week14Wt and Week22LEA, Week22LD, Week22BF, Week22Wt, respectively. Likewise, average daily gain was measured as difference in live weight from birth to week 14 (*ADGB14*), from weaning to week 14 (*ADGW14*) from week 14 to week 22 (*ADG1422*) and from week 14 to market (*ADG14MKT*). A summary of the traits employed in the current analysis is reported in Table 3.

DNA extraction and purification. Total DNA (gDNA) was extracted from each rectal swab by mechanical disruption in phenol:chloroform. Briefly, 650 μ L of extraction buffer (200 mM Tris; 200 mM NaCl; 20 mM EDTA, pH 8.0) was added to each swab stored in a 2 mL self-standing screw cap tube (Axygen, CA, USA). Tubes were shaken using a Mini-BeadBeater-96 (MBB-96; BioSpec, OK, USA) for 20 s to free sample material from the swab head. Following a brief centrifugation (10 s; 500 \times g) to pull down any dislodged material, each swab head was removed from its tube using sterile forceps. Samples were frozen solid at -80°C , and approximately 250 μ L of 0.1 mm zirconia/silica beads (BioSpec) and a 3.97 mm stainless steel ball were added to the sample (while still frozen, to avoid splashing). Samples were allowed to thaw briefly, after which 210 μ L 20% SDS and 500 μ L phenol:chloroform:IAA (25:24:1, pH 8.0) were added. Bead-beating was performed on the MBB-96 (4 min; room temperature), samples were centrifuged (3,220 \times g; 4 min), and 250 μ L of the aqueous phase was transferred to a new tube. 100 μ L of this crude DNA was then further purified using a QIAquick 96 PCR purification kit (Qiagen, MD, USA). Purification was performed per the manufacturer's instructions with the following minor modifications: (i) sodium acetate (3 M, pH 5.5) was added to Buffer PM to a final concentration of 185 mM to ensure optimal binding of genomic DNA to the silica membrane; (ii) crude DNA was combined with 4 volumes of Buffer PM (rather than 3 volumes); and, (iii) DNA was eluted in 100 μ L Buffer EB (rather than 80 μ L).

Illumina library preparation and sequencing. Phased, bi-directional amplification of the V4 region (515–806) of the 16S rRNA gene was employed to generate indexed libraries for Illumina sequencing using the strategy described by Faith *et al.*⁴⁷. Amplicon libraries were quantified using the Qubit dsDNA assay kit (Thermo Fisher Scientific Inc., MA, USA) before being pooled in equimolar ratios. These final pools were purified using Agencourt AMPure XP beads (Beckman Coulter) per the manufacturer's instructions. Purified pools were supplemented with 5–10% PhiX control DNA and were sequenced on an Illumina MiSeq machine as paired-end 2x250 + 13 bp index reactions using the 600v3 kit. Un-demultiplexed FASTQ files were generated by MiSeq Reporter. All sequencing was performed at the DNA Sequencing Innovation Lab at the Center for Genome Sciences and Systems Biology at Washington University in St. Louis.

16S rRNA gene sequencing and quality control of data. Pairs of V4 16S rRNA gene sequences were first merged into a single sequence using FLASH v1.2.11⁴⁸, with a required overlap of at least 100 and not more than 250 base pairs in order to provide a confident overlap. Sequences with a mean quality score below Q35 were then filtered out using PRINSEQ v0.20.4⁴⁹. Sequences were oriented in the forward direction and any primer sequences were matched and trimmed off; during primer matching, up to 1 mismatch was allowed. Sequences were subsequently de-multiplexed using QIIME v1.9⁵⁰. Sequences with >97% nucleotide sequence identity were then clustered into operational taxonomic units (hereafter "OTUs") using QIIME with the following settings: max_accepts = 50, max_rejects = 8, percent_subsample = 0.1 and --suppress_step4. A modified version of GreenGenes (The Greengenes Database Consortium^{51–53}) was used as the reference database. Input sequences that had 10% of the reads with no hit to the reference database were then clustered de novo with UCLUST⁵⁴ to

generate new reference OTUs to which the remaining 90% of reads were assigned. The most abundant sequence in each cluster was used as the representative sequence for the OTU. Sparse OTUs were then filtered out by requiring a minimum total observation count of 1200 for an OTU to be retained, and the OTU table was rarefied to 10,000 counts per sample. Average Good's coverage estimates for samples at weaning, week 15, and week 22, were 0.99 ± 0.002 , 0.98 ± 0.002 , and 0.98 ± 0.002 , respectively. Finally, the Ribosomal Database Project (RDP) classifier (v2.4) was retrained in the manner described in Ridaura and colleagues⁵⁵ with 0.8 cutoff used to assign taxonomy to the representative sequences. After data processing and quality control, 1755 OTUs were available for further analyses.

Statistical analysis. *Training and testing sets.* A stratified five-fold cross validation scheme was used to recursively randomly split data into training (~70% of observations) and prediction (~30% of observations) sets, maintaining equal representation of the 28 sires present in the trial. A pictorial representation of the overall experimental design is depicted in Fig. 2.

Models. All models were employed in our analysis in a regression framework. For the investigation, each combination of method, trait and time was treated as a separate analysis and accuracy of prediction for each model was obtained as the average Pearson's correlation between predicted and measured phenotypes in the test sets, similarly to what proposed in genome-wide prediction studies^{56,57}. In addition Means Squared Errors and their standard deviations were obtained.

Bayesian Lasso. For each fold/trait/time point combination two models were fitted:

A null model (*null*):

$$\mathbf{y} = \mu + \mathbf{X}\mathbf{b} + \mathbf{e}$$

where: \mathbf{y} was one of traits mentioned in the previous section, μ was a population mean, \mathbf{b} was a vector of fixed effects which included: *sex* (2 levels), *replicate* (6 levels), *sire* (28 levels), plus the covariate of weight at weaning, \mathbf{e} , was a vector of random residuals assumed $N(0, \sigma_e^2)$ and \mathbf{X} was an incidence matrix relating observations to fixed effects.

A model including the microbiome (*biom*):

$$\mathbf{y} = \mu + \mathbf{X}\mathbf{b} + \mathbf{W}\mathbf{o} + \mathbf{e}$$

where: \mathbf{o} was a vector of OTUs effects (1755 levels), \mathbf{W} was a matrix of centered and scaled OTUs counts and the remainings were as in the previous model.

We fitted the BL regression model as implemented by the R⁵⁸ package BGLR⁵⁹. OTU counts were fitted to the model with the use of a double exponential prior distribution. BGLR models double-exponential density as a mixture of scaled normal densities. In the first level of the hierarchy, marker effects are assigned independent normal densities with null mean and OTU-specific variance parameter $\tau^2 \chi \sigma_e^2$. The residual variance was assigned a scaled-inverse Chi-square prior density. BGLR provides a convenient way to choose priors shape through the R2 flag. R2 can roughly be interpreted as the expected variance proportion explained by the effect included in the model. For the residual effects default degrees of freedom of 5 were employed and an R2 of 0.60. Prior scale parameter where then obtained as $Sp = Var(y)(1 - R2)(dfp + 2)$, with Sp and dfp the scale and degrees of freedom, respectively. OTUs specific scale parameters, τ^2 are assigned IID exponential densities with rate parameter $\lambda^2/2$. The hyper parameter λ was in this case fixed and its value was assigned through a grid search on the full dataset/trait combinations (results not shown).

Random Forest. The general form of the null model employed here was (following González-Recio and Forni³⁸):

$$\mathbf{y} = \mu + \sum_{t=1}^T c_t h_t(\mathbf{y}; \mathbf{X})$$

while the biom model was:

$$\mathbf{y} = \mu + \sum_{t=1}^T c_t h_t(\mathbf{y}; \mathbf{X} + \mathbf{W})$$

Each tree $h_t(\mathbf{y}; \mathbf{X})$ or $h_t(\mathbf{y}; \mathbf{X} + \mathbf{W})$ for $t \in (1, T)$ was constructed from a random sample of the original data, and at each node a subset of features were randomly selected to create the splitting rule. Each tree was grown to the largest extent possible until all terminal nodes were maximally homogeneous³⁸. The parameter c_t is a shrinkage factor averaging the trees. The quality of split in RF can be measured through different criteria. For the current analysis mean square error (MSE) was employed. The remaining parameters of RF models in this work were set as follows: i) the number of trees was set equal to 1500; ii) the number of features to consider when looking for the best split was equal to the root of the number of original features. The bigrf package⁶⁰ of R⁵⁸ was used to fit RF models to the data.

Gradient Boosting. The general form of the null model employed here was (again following González-Recio and Forni³⁸):

$$\mathbf{y} = \mu + \sum_{m=1}^M v h_m(\mathbf{y}; \mathbf{X})$$

while the biom model was:

$$y = \mu + \sum_{m=1}^M \nu h_m(y; \mathbf{X} + \mathbf{W})$$

Each predictor $h_m(y; X)$ or $h_m(y; X + W)$ for $t \in (1, M)$ was, in this case, applied consecutively to the residual from the committee formed by the previous ones, the bagging step remaining similar to what described before. The gbm package⁶¹ of R⁵⁸ was used to fit GBM models to the data. A gaussian loss function was employed. Other parameters in the GBM models were set as follow: i) the number of trees was set equal to 1500; ii) the interaction depth was set at 3; iii) the shrinkage parameter ν was set at 0.01.

Reproducing Kernel Hilbert Space. Two RKHS models were fitted:

A null model (*null*):

$$y = \mu + \mathbf{Xb} + \mathbf{e}$$

and a (*biom*) model of form:

$$y = \mu + \mathbf{Xb} + \mathbf{Zu} + \mathbf{e}$$

where \mathbf{Z} is an incidence diagonal matrix of order (1039×1039) and \mathbf{u} is a random vector of pig effects assumed $N(0, \mathbf{M}\sigma_u^2)$. \mathbf{M} was the kernel matrix based on microbiome composition, and its computation was as follows:

microbiome was used at the OTU level to compute the Jensen-Shannon distance between pairs of samples, $D(a, b) = \sqrt{\frac{1}{2} \left(\sum_{i=1}^n a_i \log \frac{a_i}{m_i} + \sum_{i=1}^m b_i \log \frac{b_i}{m_i} \right)}$ in which $D(a, b)$ was the distance between samples a and b ; n was the number of OTUs ($n = 1755$); a_i and b_i were the counts of OTU_i in samples a and b , respectively; $m_i = (a_i + b_i)/2$ ⁶². The resulting square matrix (hereafter “JSD”) had zero on the diagonal, and values ranging between 0 and 1 on the off-diagonal. The \mathbf{M} matrix was obtained as $1 - JSD$. The RKHS regression model was implemented with the R package BGLR within a bayesian setting. Prior for σ_u^2 and σ_e^2 were chosen as highlighted in the previous section. R2 values for the the two parameters were set at 0.3 and 0.6, respectively.

Post-analysis. In order to provide a comprehensive assessment of all the factors in the design we conducted a post-analysis of the experiment with the use of a standard Linear Mixed Model (LMM). All combinations of replicate/trait/method were pooled in a single dataset. The following LMM was then fitted

$$y_{ijklm} = T_i + A_j + Tr_k + B_l + TA_{ij} + TTr_{ik} + TB_{il} + ATr_{jk} + AB_{jl} + TATrB_{ijkl} + e_{ijklm}$$

where y_{ijklm} is the accuracy of each replicate/trait/method combination; T_i is the fixed effect of the microbiome timepoint measurement (3 levels: wean, 15 wk, 22 wk); A_j is the fixed effect of the algorithm used (4 levels: BL, RKHS, RF, GBM); Tr_k is the fixed effect of the trait (12 levels: ADGBto14, ADGWto14, ADG14to22, ADG14toMKT, Week14Wt, Week14BF, Week14LD, Week14LEA, Week22Wt, Week22BF, Week22LD, Week22LEA); B_l is the fixed effect of the microbiome inclusion (2 levels: null, biom); TA_{ij} , TTr_{ik} , TB_{il} , ATr_{jk} and AB_{jl} are the pairwise interactions of the main effects; $TATrB_{ijkl}$ is the random interaction effect of T , A , Tr and B assumed $N(0, \sigma_{TATrB}^2)$; and e_{ijklm} is the random residual effects assumed $N(0, \sigma^2)$. The LMM model was fitted with the R⁵⁸ package lme4⁶³. Type III ANOVA table, least square means and contrasts were obtained with the R package lmerTest⁶⁴.

Ethics approval. Phenotypic records presented in this study came from field data. Procedures for fecal sample collection adhered to the guidelines of Institutional Animal Care and Use Committee, North Carolina State University, and National Pork Board.

Data Availability

The data that support the findings of this study are available from MATATU but restrictions apply to the availability of these data, which were used under license for the current study, and so are not publicly available. Data are however available from the authors upon reasonable request and with permission of MATATU. All scripts used for the analysis and manuscript preparation are available from the corresponding authors upon request.

References

1. Hoque, M., Kadowaki, H., Shibata, T., Oikawa, T. & Suzuki, K. Genetic parameters for measures of residual feed intake and growth traits in seven generations of duroc pigs. *Livestock Science* **121**, 45–49, <http://www.sciencedirect.com/science/article/pii/S1871141308001613> (2009).
2. Azharul, H. M. & Keiichi, S. Genetic parameters for production traits and measures of residual feed intake in duroc and landrace pigs. *Animal Science Journal* **79**, 543–549. <https://doi.org/10.1111/j.1740-0929.2008.00562.x>.
3. Jiao, S., Maltecca, C., Gray, K. A. & Cassady, J. P. Feed intake, average daily gain, feed efficiency, and real-time ultrasound traits in duroc pigs: I. genetic parameter estimation and accuracy of genomic prediction. *J. Anim. Sci.* **92**, 2377–2386, <https://doi.org/10.2527/jas.2013-7338> (2014).
4. Jiao, S., Maltecca, C., Gray, K. A. & Cassady, J. P. Feed intake, average daily gain, feed efficiency, and real-time ultrasound traits in duroc pigs: II. genomewide association. *J. Anim. Sci.* **92**, 2846–2860, <https://doi.org/10.2527/jas.2014-7337> (2014).
5. Howard, J. T. *et al.* Genome-wide association study on legendre random regression coefficients for the growth and feed intake trajectory on duroc boars. *BMC Genet.* **16**, 59, <https://doi.org/10.1186/s12863-015-0218-8> (2015).
6. Jiao, S., Tiezzi, F., Huang, Y., Gray, K. A. & Maltecca, C. The use of multiple imputation for the accurate measurements of individual feed intake by electronic feeders. *J. Anim. Sci.* **94**, 824–832, <https://doi.org/10.2527/jas.2015-9667> (2016).
7. Lu, D. *et al.* The relationship between different measures of feed efficiency and feeding behavior traits in duroc pigs1. *J. Anim. Sci.* **95**, 3370–3380, <https://doi.org/10.2527/jas.2017.1509> (2017).

8. J.J., C. & T., T. Optimized management of genetic variability in selected pig populations. *Journal of Animal Breeding and Genetics* **125**, 291–300. <https://doi.org/10.1111/j.1439-0388.2008.00738.x>.
9. Howard, J. T., Pryce, J. E., Baes, C. & Maltecca, C. Invited review: Inbreeding in the genomics era: Inbreeding, inbreeding depression, and management of genomic variability. *J. Dairy Sci.* **100**, 6009–6024 (2017).
10. Brestoff, J. R. & Artis, D. Commensal bacteria at the interface of host metabolism and the immune system. *Nat. Immunol.* **14**, 676 (2013).
11. Pflughoeft, K. J. & Versalovic, J. Human microbiome in health and disease. *Annual Review of Pathology: Mechanisms of Disease* **7**, 99–122 (2012).
12. Gill, S. R. *et al.* Metagenomic analysis of the human distal gut microbiome. *Science* **312**, 1355–1359 (2006).
13. Metzler-Zebeli, B. U. *et al.* Adaptation of the cecal bacterial microbiome of growing pigs in response to resistant starch type 4. *Appl. Environ. Microbiol.* **81**, 8489–8499 (2015).
14. Niu, Q. *et al.* Dynamic distribution of the gut microbiota and the relationship with apparent crude fiber digestibility and growth stages in pigs. *Sci. Rep.* **5**, 9938 (2015).
15. Jayaraman, B. & Nyachoti, C. M. Husbandry practices and gut health outcomes in weaned piglets: A review. *Animal Nutrition* **3**, 205–211 (2017).
16. Moeser, A. J., Pohl, C. S. & Rajput, M. Weaning stress and gastrointestinal barrier development: Implications for lifelong gut health in pigs. *Animal Nutrition* (2017).
17. Kim, J., Hansen, C. F., Mullan, B. & Pluske, J. Nutrition and pathology of weaner pigs: Nutritional strategies to support barrier function in the gastrointestinal tract. *Animal Feed Science and Technology* **173**, 3–16 (2012).
18. Bian, G. *et al.* Age, introduction of solid feed and weaning are more important determinants of gut bacterial succession in piglets than breed and nursing mother as revealed by a reciprocal cross-fostering model. *Environ. Microbiol.* **18**, 1566–1577 (2016).
19. Lu, D. *et al.* Host contributes to longitudinal diversity of fecal microbiota in swine selected for lean growth. *Microbiome* **6**, 4 (2018).
20. Morota, G., Ventura, R., Silva, F., Koyama, M. & Fernando, S. Machine learning and data mining advance predictive big data analysis in precision animal agriculture. *Journal of Animal Science* (2018).
21. De Los Campos, G. *et al.* Predicting quantitative traits with regression models for dense molecular markers and pedigree. *Genetics* **182**, 375–385 (2009).
22. Liaw, A. *et al.* Classification and regression by randomforest. *R news* **2**, 18–22 (2002).
23. Friedman, J. H. Greedy function approximation: a gradient boosting machine. *Annals of statistics* 1189–1232 (2001).
24. De Los Campos, G., Gianola, D. & Rosa, G. J. Reproducing kernel hilbert spaces regression: a general framework for genetic evaluation. *J. Anim. Sci.* **87**, 1883–1887 (2009).
25. He, M. *et al.* Evaluating the contribution of gut microbiota to the variation of porcine fatness with the cecum and fecal samples. *Front. Microbiol.* **7**, 2108, <https://doi.org/10.3389/fmicb.2016.02108> (2016).
26. Fang, S., Xiong, X., Su, Y., Huang, L. & Chen, C. 16s rna gene-based association study identified microbial taxa associated with pork intramuscular fat content in feces and cecum lumen. *BMC. Microbiol.* **17**, 162 (2017).
27. McCormack, U. M. *et al.* Exploring a possible link between the intestinal microbiota and feed efficiency in pigs. *Applied and environmental microbiology* **83**, <http://europepmc.org/articles/PMC5514681> (2017).
28. Yang, H. *et al.* Unraveling the fecal microbiota and metagenomic functional capacity associated with feed efficiency in pigs. *Front. Microbiol.* **8**, 1555, <https://doi.org/10.3389/fmicb.2017.01555> (2017).
29. Ramayo-Caldas, Y. *et al.* Phylogenetic network analysis applied to pig gut microbiota identifies an ecosystem structure linked with growth traits. *ISME. J.* **10**, 2973 (2016).
30. Cole, J. B. *et al.* Genome-wide association analysis of thirty one production, health, reproduction and body conformation traits in contemporary us holstein cows. *BMC Genomics* **12**, 408 (2011).
31. Camarinha-Silva, A. *et al.* Host genome influence on gut microbial composition and microbial prediction of complex traits in pigs. *Genetics* **206**, 1637–1644, <http://www.genetics.org/content/206/3/1637>, <https://doi.org/10.1534/genetics.117.200782> (2017).
32. Tiezzi, F., De Los Campos, G., Gaddis, K. P. & Maltecca, C. Genotype by environment (climate) interaction improves genomic prediction for production traits in us holstein cattle. *J. Dairy Sci.* **100**, 2042–2056 (2017).
33. Lopez-Cruz, M. *et al.* Increased prediction accuracy in wheat breeding trials using a marker × environment interaction genomic selection model. *G3: Genes, Genomes, Genetics* **g3**–114 (2015).
34. Gianola, D., De Los Campos, G., Hill, W. G., Manfredi, E. & Fernando, R. Additive genetic variability and the bayesian alphabet. *Genetics* **183**, 347–363 (2009).
35. Gianola, D. & van Kaam, J. B. Reproducing kernel hilbert spaces regression methods for genomic assisted prediction of quantitative traits. *Genetics* **178**, 2289–2303 (2008).
36. De Los Campos, G., Gianola, D., Rosa, G. J., Weigel, K. A. & Crossa, J. Semi-parametric genomic-enabled prediction of genetic values using reproducing kernel hilbert spaces methods. *Genetics Research* **92**, 295–308 (2010).
37. Breiman, L. Random forests. *Machine learning* **45**, 5–32 (2001).
38. González-Recio, O. & Forni, S. Genome-wide prediction of discrete traits using bayesian regressions and machine learning. *Genet. Sel. Evol.* **43**, 7 (2011).
39. Crossa, J. *et al.* Genomic prediction in cimmyt maize and wheat breeding programs. *Heredity* **112**, 48 (2014).
40. Morota, G. & Gianola, D. Kernel-based whole-genome prediction of complex traits: a review. *Front. Genet.* **5**, 363 (2014).
41. González-Recio, O., Rosa, G. J. & Gianola, D. Machine learning methods and predictive ability metrics for genome-wide prediction of complex traits. *Livestock Science* **166**, 217–231 (2014).
42. Pasolli, E., Truong, D. T., Malik, F., Waldron, L. & Segata, N. Machine learning meta-analysis of large metagenomic datasets: tools and biological insights. *PLoS Comput. Biol.* **12**, e1004977 (2016).
43. Chang, H.-X., Haudenschild, J. S., Bowen, C. R. & Hartman, G. L. Metagenome-wide association study and machine learning prediction of bulk soil microbiome and crop productivity. *Front. Microbiol.* **8**, 519 (2017).
44. Maltecca, C. *et al.* Metagenomic predictions of growth and carcass traits in pigs with the use of bayesian alphabet and machine learning methods. *Proceedings, 10th World Congress of Genetics Applied to Livestock Production. Auckland, New Zealand Feb10–16* (2018).
45. Xiao, L. *et al.* A reference gene catalogue of the pig gut microbiome. *Nature microbiology* **1**, 16161 (2016).
46. Lu, D. *et al.* Contribution of microbiome to variation in fat and growth traits in crossbred pigs. *Proceedings, 10th World Congress of Genetics Applied to Livestock Production. Auckland, New Zealand Feb10–16* (2018).
47. Faith, J. J. *et al.* The long-term stability of the human gut microbiota. *Science* **341**, 1237439 (2013).
48. Magoč, T. & Salzberg, S. L. Flash: fast length adjustment of short reads to improve genome assemblies. *Bioinformatics* **27**, 2957–2963 (2011).
49. Schmieder, R. & Edwards, R. Quality control and preprocessing of metagenomic datasets. *Bioinformatics* **27**, 863–864 (2011).
50. Caporaso, J. G. *et al.* Qiime allows analysis of high-throughput community sequencing data. *Nat. Methods* **7**, 335 (2010).
51. [greengenes.secondgenome.com, http://greengenes.secondgenome.com/downloads/database/13_5](http://greengenes.secondgenome.com/downloads/database/13_5).
52. Schloss, P. D. & Handelsman, J. Toward a census of bacteria in soil. *PLoS Comput. Biol.* **2**, e92 (2006).
53. Ley, R. E., Turnbaugh, P. J., Klein, S. & Gordon, J. I. Microbial ecology: human gut microbes associated with obesity. *Nature* **444**, 1022 (2006).
54. Edgar, R. C. Search and clustering orders of magnitude faster than blast. *Bioinformatics* **26**, 2460–2461 (2010).

55. Ridaura, V. K. *et al.* Gut microbiota from twins discordant for obesity modulate metabolism in mice. *Science* **341**, 1241214 (2013).
56. Tiezzi, F. & Maltecca, C. Accounting for trait architecture in genomic predictions of us holstein cattle using a weighted realized relationship matrix. *Genet. Sel. Evol.* **47**, 24, <https://doi.org/10.1186/s12711-015-0100-1> (2015).
57. Gray, K. A., Cassady, J. P., Huang, Y. & Maltecca, C. Effectiveness of genomic prediction on milk flow traits in dairy cattle. *Genet. Sel. Evol.* **44**, 24, <https://doi.org/10.1186/1297-9686-44-24> (2012).
58. Team, R. C. R: A language and environment for statistical computing (2018).
59. Pérez, P. & de Los Campos, G. Genome-wide regression & prediction with the bglr statistical package. *Genetics* genetics–114 (2014).
60. Lim, A., Breiman, L. & Cutler, A. bigrf: Big random forests: Classification and regression forests for large data sets, <http://cran.r-project.org/package=bigrf> (2014).
61. Ridgeway, G. Generalized boosted models: A guide to the gbm package, <http://cran.r-project.org/package=gbm>.
62. Endres, D. M. & Schindelin, J. E. A new metric for probability distributions. *IEEE Transactions on Information theory* **49**, 1858–1860 (2003).
63. Bates, D., Mächler, M., Bolker, B. & Walker, S. Fitting linear mixed-effects models using lme4. *arXiv preprint arXiv:1406.5823* (2014).
64. Kuznetsova, A., Brockhoff, P. B. & Christensen, R. H. B. Package 'lmerTest'. *R package version 2* (2015).

Acknowledgements

We would like to thank Jessica Hoisington-Lopez from the DNA sequencing Innovation Lab at the Center for Genome Sciences and Systems Biology at Washington University in St. Louis for her sequencing expertise and Nicholas S. Grohmann for phenotype and sample collection. This study is a part of the project “Re-defining growth efficiency accounting for the interaction between host genome and commensal gut bacteria” funded by The National Pork Board Association and is part of the project “From Host to Guest and Back” funded by the Maschhoffs, LLC and North Carolina State University.

Author Contributions

C.M. designed and carried out the analyses and drafted the manuscript. C.S. and N.M. were responsible for sequencing and bioinformatic work, as well as drafting related sections in the “Methods” section. F.T. and D.L. were involved in designing the experiment and providing consultation for the analyses. All co-authors provided comments for the manuscript. C.M. directed the overall research project. All authors have read and approved the final manuscript.

Additional Information

Supplementary information accompanies this paper at <https://doi.org/10.1038/s41598-019-43031-x>.

Competing Interests: The authors declare no competing interests.

Publisher’s note: Springer Nature remains neutral with regard to jurisdictional claims in published maps and institutional affiliations.



Open Access This article is licensed under a Creative Commons Attribution 4.0 International License, which permits use, sharing, adaptation, distribution and reproduction in any medium or format, as long as you give appropriate credit to the original author(s) and the source, provide a link to the Creative Commons license, and indicate if changes were made. The images or other third party material in this article are included in the article’s Creative Commons license, unless indicated otherwise in a credit line to the material. If material is not included in the article’s Creative Commons license and your intended use is not permitted by statutory regulation or exceeds the permitted use, you will need to obtain permission directly from the copyright holder. To view a copy of this license, visit <http://creativecommons.org/licenses/by/4.0/>.

© The Author(s) 2019